Airborne Radar Simulation with Adaptive Antenna Techniques

M92B0000083
July 1992

B. N. Suresh Babu
J. A. Torres

MITRE
Bedford, Massachusetts

Airborne Radar Simulation with Adaptive Antenna Techniques

M92B0000083
July 1992

B. N. Suresh Babu
J. A. Torres

Contract Sponsor MTC
Contract No. N/A
Project No. 021D
Dept. D085

MITRE
Bedford, Massachusetts

Department Approval: 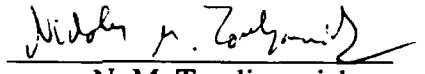

N. M. Tomljanovich

MITRE Project Approval: 

C. H. Gager

REPORT DOCUMENTATION PAGE

Form Approved
OMB No. 0704-0188

1. AGENCY USE ONLY *(Leave blank)*	2. REPORT DATE	3. REPORT TYPE AND DATES COVERED
	July 1992	

4. TITLE AND SUBTITLE

Airborne Radar Simulation with Adaptive Antenna Techniques

5. FUNDING NUMBERS

PR

6. AUTHOR(S)

B.N. Suresh Babu
J. A. Torres

7. PERFORMING ORGANIZATION NAME(S) AND ADDRESS(ES)

The MITRE Corporation
202 Burlington Road
Bedford, MA 01730-1420

8. PERFORMING ORGANIZATION REPORT NUMBER

M92B0000083

9. SPONSORING / MONITORING AGENCY NAME(S) AND ADDRESS(ES)

N/A

10. SPONSORING / MONITORING AGENCY REPORT NUMBER

N/A

11. SUPPLEMENTARY NOTES

12a. DISTRIBUTION / AVAILABILITY STATEMENT

Approved for public release;
distribution unlimited

12b. DISTRIBUTION CODE

13. ABSTRACT *(Maximum 200 words)*

This document presenta a reprint of a conference paper given at the Summer Computer Simulation Conference (SCSC) held in Reno, Nevada. It describes a flexible general airborne radar simulation with adaptive space-time processing (STP) antenna techniques for clutter and jammer suppression. This paper presenta parametric performance curves for different array configurations and different suboptimal STP architectures.

14. SUBJECT TERMS

SCSC, Airborne radar simulation, adaptive space-time processing, clutter and jammer suppression, parametric performance curves

15. NUMBER OF PAGES

9

16. PRICE CODE

17. SECURITY CLASSIFICATION OF REPORT	18. SECURITY CLASSIFICATION OF THIS PAGE	19. SECURITY CLASSIFICATION OF ABSTRACT	20. LIMITATION OF ABSTRACT
Unclassified	Unclassified	Unclassified	

PREFACE

This document presents a reprint of a conference paper given at the Summer Computer Simulation Conference (SCSC) held in Reno, Nevada on 27-29 July 1992. This paper describes a flexible general airborne radar simulation with adaptive space-time processing (STP) antenna techniques for clutter and jammer suppression. The program is an end-to-end performance simulation allowing assessment of the capability and limitations of adaptive arrays for clutter and jammer suppression, and sizing of different optimum and suboptimum adaptive antenna configurations. This paper presents parametric performance curves for different array configurations and different suboptimal STP architectures.

AIRBORNE RADAR SIMULATION WITH ADAPTIVE ANTENNA TECHNIQUES

B. N. Suresh Babu and J. A. Torres
The MITRE Corporation
Burlington Road
Bedford, MA 01730-0208

ABSTRACT

The surface clutter problem associated with moving airborne radars is more serious than for ground-based radars because of the wide Doppler spread of the sidelobe clutter returns which encompass the Doppler frequency of the target. One of the methods for detecting targets in clutter that has both a spatial and Doppler spread is to use space-time processing (STP). To gain insight into one of the space-time architectures, jointly adaptive STP, which employs the joint processing of array elements and pulse train data, we developed a flexible general airborne radar simulation using adaptive antenna techniques. The program is an end-to-end performance simulation which includes aircraft motion and platform crab angle effects; adaptive STP; radar and waveform parameters; and target, clutter, and jammer models. The program incorporates modeling of internal clutter motion (ICM), bandwidth, and channel mismatching (CM). It allows assessment of the capability and limitations of adaptive arrays for clutter and jammer interference suppression, and sizing of different optimum and suboptimum (subarraying and beam space) adaptive antenna configurations. This paper describes the simulation and presents parametric performance curves for different array configurations (side- and forward-looking) and different suboptimal STP architectures.

INTRODUCTION

New surveillance radars for strategic and tactical applications are needed to detect targets with very low radar cross sections. This requires a large power-aperture product which, in turn, increases the level of the clutter and jammer signals received from the antenna sidelobe region. Receiving antennas with ultra-low sidelobe patterns and adaptive sidelobe cancellers have been proposed for large phased-array radars to suppress these interference signals. However, MITRE identified limitations in these techniques for achieving the required interference signal suppression and developed a flexible simulation to evaluate the capabilities of proposed designs.

The objective of this paper is to describe features of a simulation tool which will enable us to evaluate advanced airborne radars with adaptive antenna techniques (STP) (Brennan and Reed 1973; Klem 1983; Barile et al. 1991). The software includes the calculation of radar performance in jamming and clutter scenarios and models STP for both jamming and clutter suppression. For a large phased-array antenna, the limitations of a practical implementation of optimal STP will in general require suboptimal architectures such as beam space and subarraying. The radar software enables system engineers to perform complexity versus performance trade-offs relative to the optimal STP for these implementations. The software has been implemented on VMS- and UNIX-based machines using FORTRAN.

STP, the adaptive joint processing of array element and pulse train data, adaptively reduces the sidelobe clutter to enhance detectability of targets. As shown in figure 1, the spread of mainbeam clutter for an airborne radar is small, limited by the angle extent of the mainbeam, but the spread of sidelobe clutter is greater, as shown in figure 2. The conventional technique of Doppler filtering is ineffective because sidelobe clutter echoes have the same Doppler as low velocity targets. However, STP allows discrimination between the target and the sidelobe clutter by using joint information in the two dimensions (azimuth (i.e., space) and Doppler (i.e., time)) to process the data. Figure 3 illustrates a three-dimensional (3-D) azimuth-Doppler antenna gain pattern which shows that STP cancels the clutter by placing a notch along the locations of the scatterers. The optimal STP (see figure 4) filter is formed by placing a tapped delay line at the output of each element or subarray of the antenna array, with the taps spaced by one pulse repetition interval (PRI). The number of PRI taps (i.e., pulses) equals the number of outputs to be coherently processed. Optimal weights for each of these taps are derived from assumptions about the location and Doppler of the target and the clutter. Each weight is applied to the appropriate PRI tap, and the resulting weighted outputs are summed, providing a coherent combination of information from each element and PRI. The resultant sum maximizes both the output signal-to-interference ratio (SIR) and the probability of detection while maintaining a constant false alarm rate. This sum is tested against a threshold criterion to determine if the target is absent or present.

The computational complexity of STP is a significant consideration in practical implementations, but it can be reduced by using suboptimal approaches while still

maintaining performance close to optimal. There are many variations of this scheme involving the criterion of optimality used, methods for computing the optimal weights, and hybrids of fixed and adaptive Doppler processing. The suboptimal approaches reduce the complexity of implementation by decreasing the number of degrees of freedom. One suboptimal version, the jointly adaptive approach using element space processing employs significantly fewer adaptive pulses than the number of outputs to be coherently processed, constituting the number of elements times the number of pulses degrees of freedom. A second version, the jointly adaptive approach using beam space processing, employs non-adaptive beamforming of the array elements to form distinct beams that provide the spatial (or azimuth) information required by the two-dimensional STP. The number of beams is significantly less than the number of elements, constituting the number of beams times the number of pulses degrees of freedom. A third version, the jointly-adaptive approach using subarraying, employs non-adaptive subarraying of the array elements to provide the spatial information. The number of subarrays is significantly less than the number of elements, constituting the number of subarrays times the number of pulses degrees of freedom. All three suboptimal approaches include a Doppler processor following the STP summation output to provide further coherent gain.

One of the critical issues in subarraying is the generation of grating lobes in the antenna pattern due to the large phase center separation between the subarrays. The program has the capability to investigate the effects of subarray overlapping on the performance of STP. In the beam space architecture, a feature selects only a few specified beams which receive maximum jamming power, enabling us to perform parametric studies of performance using fewer degrees of freedom. The software models moving target indicator (MTI) filtering preprocessing which reduces the dynamic range requirements for the architectures, so we can evaluate the performance of the adaptive processor due to the preprocessor.

Figure 5 shows a global flow of the simulation which has two modes — non-adaptive and adaptive. To keep the software architecture general, in both modes the program computes the covariances matrices for the clutter, signal, jamming, and thermal noise, based on the expected values (i.e., steady-state) of signal and interference parameters. The program uses the adaptive or non-adaptive weights in conjunction with the covariance matrices to compute various performance measures.

Using the radar system input parameters, the program computes the clutter-plus-noise-to-noise ratio (CNR) for each radar resolution cell and determines the Doppler frequency at the center of the cell. The clutter is then summed across each range ring applying the antenna pattern gain. Range folding is accounted for by summing over each range ring that folds over the selected pulse repetition frequency (PRF). The Doppler ambiguities are also included in the simulation. Since it is a constant Gamma clutter model, it gives a clutter unit backscatter coefficient that is a function of grazing angle. The system losses are divided into categories of range-independent losses which are common losses for clutter, jamming, and target; target-only losses; and range-dependent losses for the clutter and target. This allows us to calculate performance as a function of range in a clutter background. The program computes the atmospheric losses as a function of range. Elevation beamshape loss is computed in the program based on the assumed antenna pattern and depression angle. We can generate the CNR, SIR, signal-to-noise ratio (SNR), and jammer-plus-noise-to-noise ratio (JNR) as a function of Doppler frequency.

Non-Adaptive and Adaptive Weights Computation

In the non-adaptive mode, the weights are given by the specified spatial antenna beamforming and MTI filtering weights. The adaptive weights are computed by multiplying the inverse of the sum of the covariance matrices with a steering vector. The steering vector (Brennan and Reed 1973) is tuned for a hypothesized target that is at a particular azimuth and Doppler. The corresponding steering vectors for the suboptimal architectures are calculated by performing the appropriate transformations used on the input signal and interference element data.

The software has the capability to study the effect of channel equalization on mitigating the channel mismatch effects on the overall performance. If the channel mismatch limitations are caused by slowly varying circuit parameters, then the equalization filter weights can be computed prior to adaptive processing. However, if they are caused by dispersive antenna errors or jammer multipath, the weights must be an integral part of an adaptive weight computation. The software incorporates equalization filter weights as an integral part of adaptive weight computation wherein the degrees of freedom are equal to the number of taps times the number of pulses times the number of elements, beams, or subarrays.

Received Signals

The received clutter signal is simulated by placing range rings of clutter scatterers at closely spaced azimuth intervals and summing the two-way clutter return from each scatterer independently. Returns from several frequencies within the bandwidth of the compressed transmitted pulse are summed to include the effects of bandwidth. The simulation incorporates all range and Doppler ambiguous clutter based on the PRF of the transmitted waveform and the array geometry. The complex amplitude of any frequency return associated with a scatterer is calculated from the frequency of the return,

transmit antenna pattern, range, backscatter coefficient, element receive pattern, and elevation receive antenna pattern. The phase of the return includes the initial delay of the clutter echo, Doppler phase shift due to aircraft motion, and azimuth phase shift due to the scatterer location relative to the array broadside. The reflected power from the scatterer returns in each ambiguous range ring is calculated from the radar range equation.

The target is assumed to be a single far-field scatterer at a specified range, consisting of several frequency returns within the bandwidth of the compressed transmitted pulse. The complex amplitude and phase terms used to describe the target received signal are equivalent to those describing the clutter, and include the Doppler shift due to the target motion. The target model is a constant sigma model.

The received noise-like jamming signal consists of several frequency returns from jammers located in the far-field. The complex amplitude of any frequency return associated with a jammer is computed from the frequency of the return, element receive pattern, elevation receive antenna pattern, and the effective radiated power. The calculation of the phase term of the jammer return is similar to the method used for the clutter.

The thermal noise power received at an antenna element is calculated from the product of Boltzmann's constant, the standard system temperature, the compressed transmitted pulse bandwidth, and the system noise figure.

ICM and CM Models

To model the ICM, the clutter steady-state covariance matrix is modified by multiplying any product of the pulse-to-pulse delayed scatterer returns by a decorrelation coefficient that is a function of their difference in delay, the radar center frequency, and the root mean square value of the ICM. The CM between array elements determines the ability to provide adequate nulling of jammers and clutter. The off-diagonal entries of the interference and signal covariance matrices are modified to incorporate the effects of CM errors by including the multiplicative element-to-element decorrelation coefficient.

Pattern Distortion and Eigenvalue Compensation

For two-pulse STP, ICM and aircraft crab angle can distort the adapted antenna pattern by significantly degrading its peak and sidelobes, causing signal cancellation. Eigenvalue compensation using singular value decomposition is used in the simulation to mitigate the effects of pattern distortion (Barile et al. 1991).

Performance Measures

The software computes the expected power at the output of the summation and at any Doppler filter output for the clutter, jammer, noise, and target from the (adaptive or non-adaptive) weights and the individual covariance matrices. The various performance measures are calculated by forming any desired ratio of expected output powers for the signal components. Performance measures at each Doppler cell are calculated by varying the target Doppler. In the adaptive mode, the STP weights are fixed for a target hypothesized at a particular Doppler, and are not optimal for other target Dopplers. In either mode, the quiescent performance is also evaluated using the quiescent weights (i.e., same spatial weights used on transmit).

Antenna Gain Patterns and Eigenspectrum Analysis

Additional insight into performance can be obtained by plotting the 3-D non-adapted and adapted antenna gain patterns at different azimuths and normalized Dopplers (see figure 3), and also from the eigenspectrum analysis of the interference covariance matrix (Barile et al. 1991). The software evaluates 3-D patterns by calculating the output power when a test target is at different azimuths and normalized Dopplers. In addition, the software evaluates the quiescent antenna gain pattern and principal plane antenna patterns. It generates the eigenvalues from the interference covariance matrix. The eigenvalues are normalized such that the largest eigenvalue equals unity.

Results

We present four examples to show various aspects of the simulation. The first and second examples show that the simulation can be used for determining the cancellation ratio requirements for the phased-array radar to have adequate jammer nulling capability, and illustrate the effect of radar bandwidth on the jammer nulling capability. The third example illustrates the radar performance for different antenna configurations, the side- and forward-looking arrays. The final example illustrates the performance of two different STP architectures, subarray and beam space. For conciseness, the specific parameters and performance measures for all of the examples are included in the figures.

Example 1

Figure 6 illustrates the effect of CM on the adapted signal-to-jammer-plus-noise ratio (SJNR) for a 50-column array using one-pulse STP for various values of cancellation ratio ranging from 30 to 90 dB. The jammer is located in azimuth at 20 degrees relative to broadside. With perfect matching the adapted SJNR improves to the maximum value (i.e., adapted SNR). In addition, the adapted SJNR deteriorates linearly with the inverse of the cancellation

ratio when CM is significant. To maintain a loss of less than 3 dB in output SJNR, a cancellation ratio of 70 dB is required for this example. Figure 7 is a plot of the normalized eigenvalues of the jammer-plus-noise covariance matrix for three cases of CM: cancellation ratios equal to 90, 45, and 35 dB. It shows that CM increases the lowest eigenvalues compared with the case of perfect matching. The results show that significant levels of CM (i.e., when the lowest eigenvalue due to CM is greater than the noise power) affect the null depth (proportional to cancellation ratio) at the jammer location, as illustrated in figure 8, where the adapted patterns are evaluated only at azimuth angles near the jammer location.

Example 2

We illustrate the effect of radar receiver bandwidth (BW) on the nulling capability of multiple noise-like jammers (eight) located in the sidelobes of a 15-element linear array. Figure 9 illustrates the effect of bandwidth on the residual JNR for various values of BW. As the BW increases, so does the jammer BW, which increases the jammer residual and degrades the system performance. Figure 10 is a plot of normalized eigenvalues of the jammer-plus-noise covariance matrix for three different BWs. For narrowband jamming, there are eight dominant eigenvalues requiring eight degrees of freedom to mitigate the jammers. However, for wideband jamming the number of dominant eigenvalues is greater than 15. Since the system has only 15 degrees of freedom, it causes performance degradation. Increasing the spatial or temporal degrees of freedom can mitigate the reduction in performance due to the wideband jamming.

Example 3

Here, we present the effects of two antenna configurations on the system performance using two-pulse STP for a 50-column array. Note that the forward-looking array performance is simulated using a side-looking array with an aircraft azimuth crab angle of 90 degrees. Aircraft crab angle causes a Doppler displacement of the spatial location of each clutter scatterer and results in pattern distortion and degradation in adapted signal-to-clutter-plus-noise ratio (SCNR). The pattern distortion is alleviated by using eigenvalue compensation. Figure 11 illustrates that the lowest eigenvalue for the forward-looking array increases by 60 dB compared to the side-looking array degrading the output SCNR. However, by processing more pulses the performance degradation of the forward-looking array can be mitigated.

Example 4

To illustrate the subarray architecture, we use a 15-element linear array with three sidelobe jammers and five subarrays. Figure 12 shows the quiescent and adapted antenna patterns. The adapted pattern has three nulls in the direction of the three jammers. In addition, there is a grating null in the mainbeam due to one of the jammers located in one of the grating lobes. The software has the capability to overcome the grating lobe problems by using subarray overlapping.

Figure 13 is a plot of adapted SIR as a function of the number of beams adaptively processed (NBEAMS) for a 20-element linear array with urban clutter and three sidelobe jammers. The beams processed are a combination of the beams clustered around the look direction (NC) and the remaining beams (NBEMS-NC) that are selected based on the maximum received jamming power. For this example, the performance curves show that reducing the degrees of freedom using suboptimal beam space processing can achieve near optimal performance, but it is dependent on how the beams are selected.

Summary

The flexible simulation tool described in this paper allows system engineers to evaluate the performance of airborne phased-array radar systems with STP techniques for clutter and jamming suppression. Using the program, design engineers can perform parametric studies by varying the antenna, radar system, and environmental parameters (i.e., clutter and jamming scenarios), and can compare the performance with and without adaptive STP techniques. In addition, system engineers can perform complexity versus performance trade-offs relative to optimal STP for three different suboptimal architectures. The examples described in this paper illustrate several key features of the simulation.

List of References

1. Brennan, L.E. and I.S. Reed. 1973. "Theory of Adaptive Radar," *IEEE Transactions on Aerospace and Electronic Systems*, AES-9.

2. Klemm, R. 1983. "Adaptive Clutter Suppression for Airborne Phased-Array Radars," *IEE Proceedings*, Vol. 130.

3. Barile, E.C.; R.L. Fante; B.N. Suresh Babu; and J.A. Torres. 1991. "Some Limitations on Space-Time Processing in Reducing Airborne Clutter," *Progress in Electromagnetic Research Symposium.*

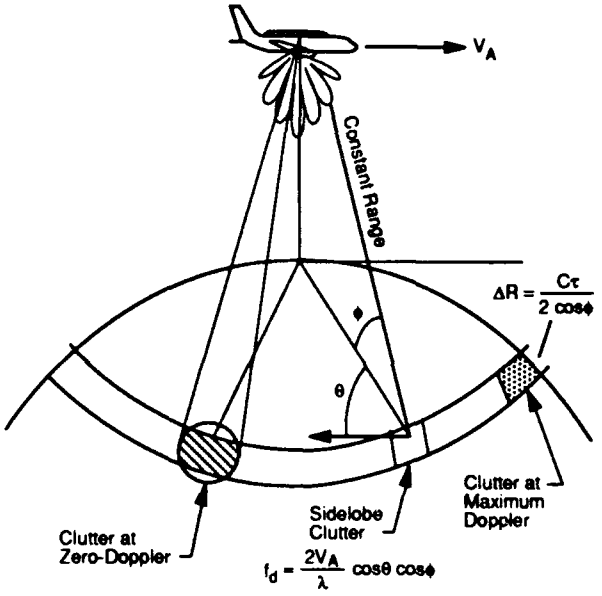

Figure 1. Airborne Radar Clutter

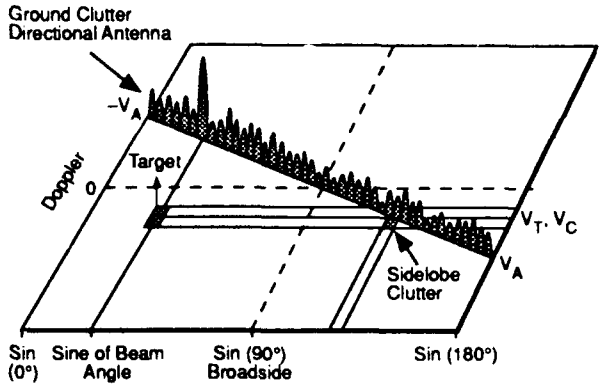

Figure 2. Angle-Doppler Plot of Airborne Radar Clutter

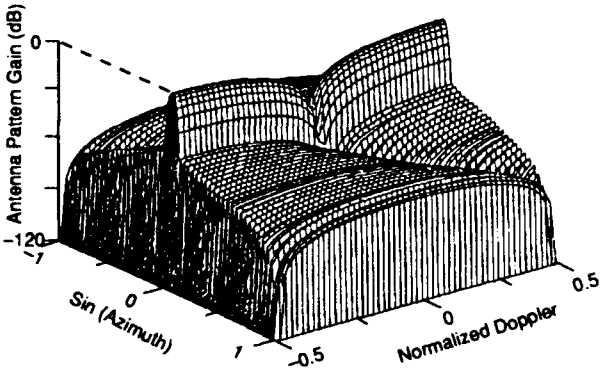

Figure 3. Example of Adapted Antenna Gain Pattern

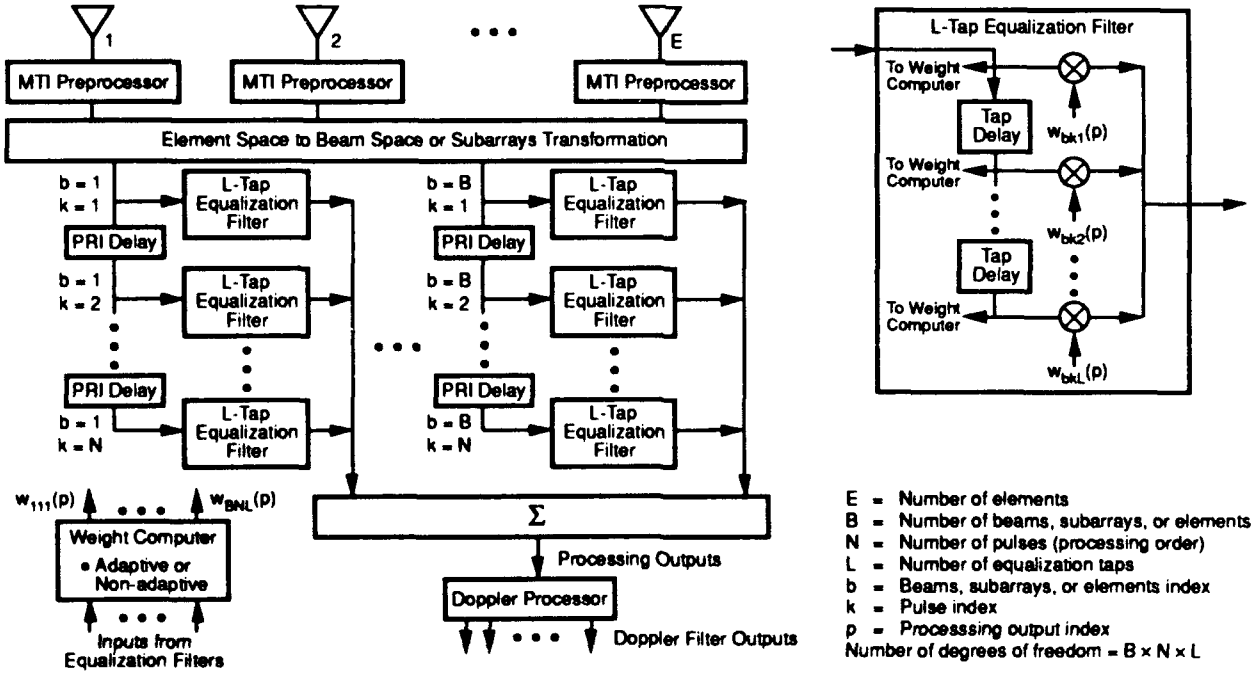

Figure 4. Adaptive and Non-Adaptive Processing Architecture

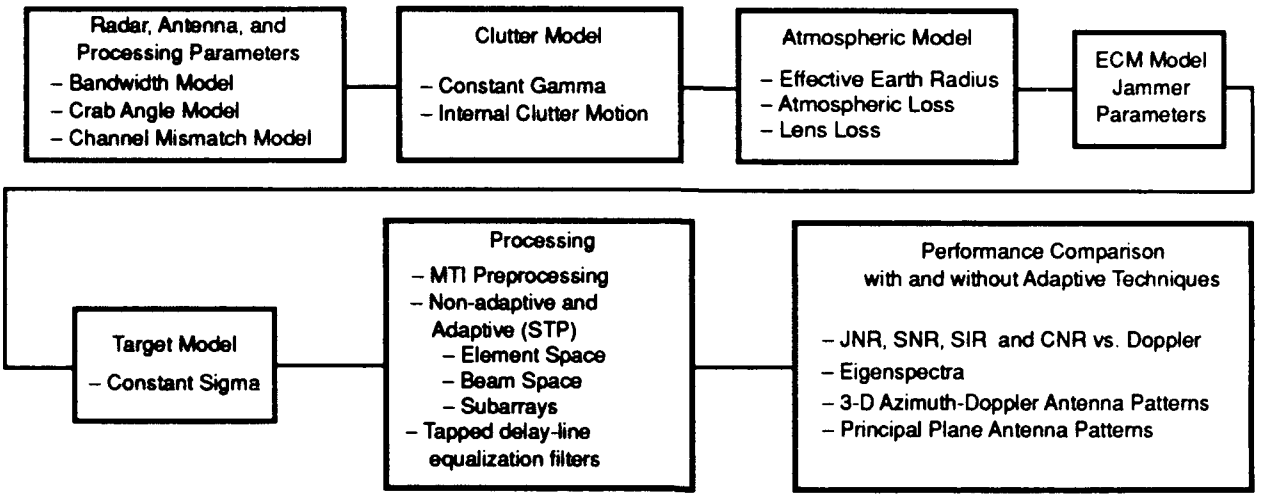

Figure 5. Global Flow of Airborne Radar Simulation

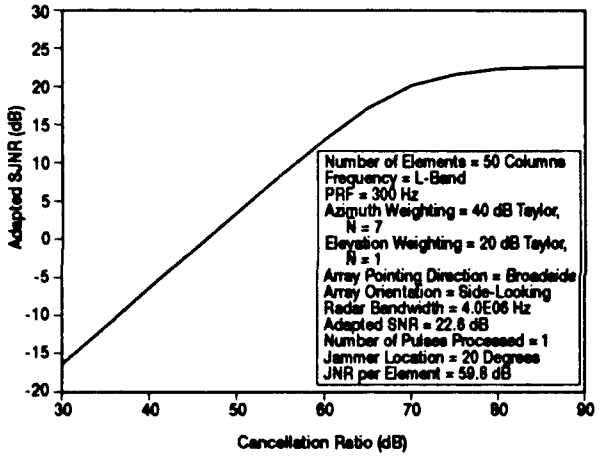

Figure 6. Effect of Channel Mismatch on Adapted Signal-to-Jammer-Plus-Noise Ratio

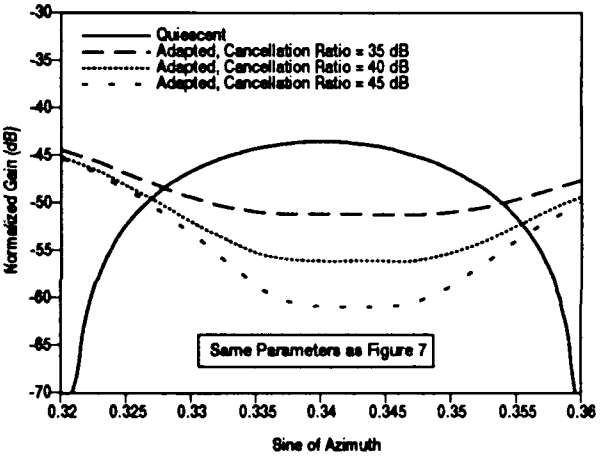

Figure 8. Effect of Channel Mismatch on Jammer Null Depth

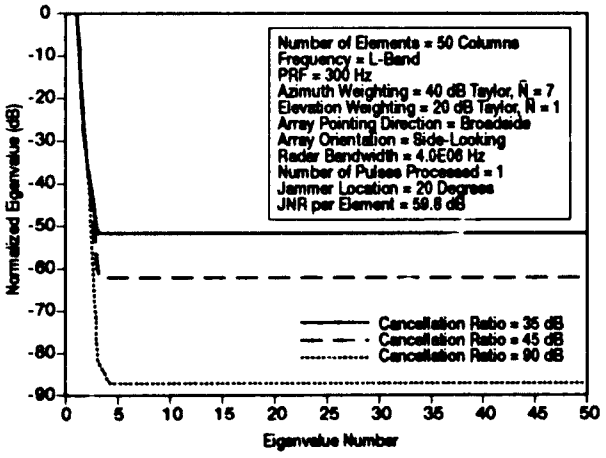

Figure 7. Effect of Channel Mismatch on Jammer-Plus-Noise Eigenvalues

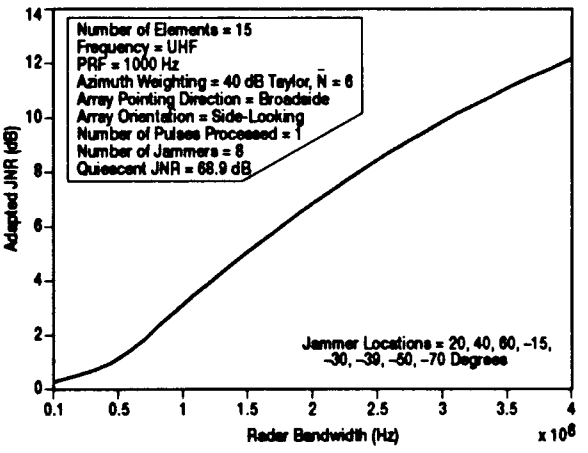

Figure 9. Effect of Radar Bandwidth on Adapted Jammer-Plus-Noise-to-Noise Ratio

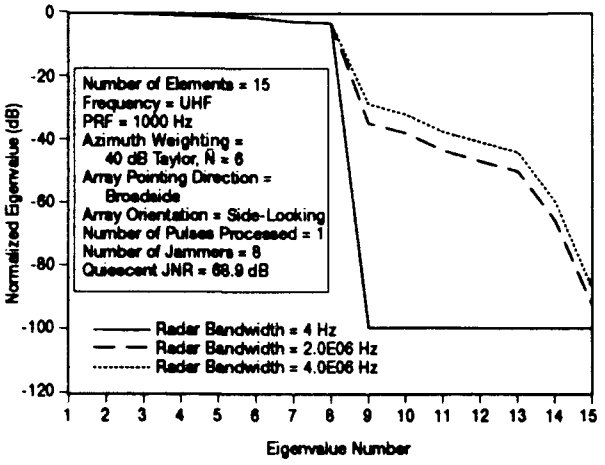

Figure 10. Effect of Radar Bandwidth on Jammer-Plus-Noise Eigenvalues

Parameter	Adapted, Two-pulse STP		
	Quiescent	Side-Looking	Forward-Looking
SCNR in dB	-55.1	25.6	-32.7
SNR in dB	22.6	25.6	25.6

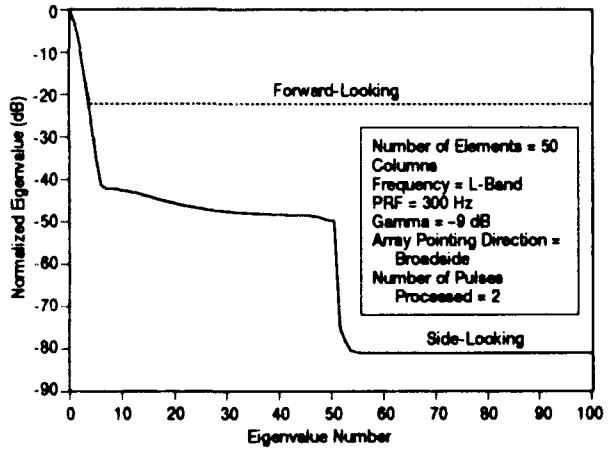

Figure 11. Effect of Array Orientation on Clutter-Plus-Noise Eigenvalues and Performance

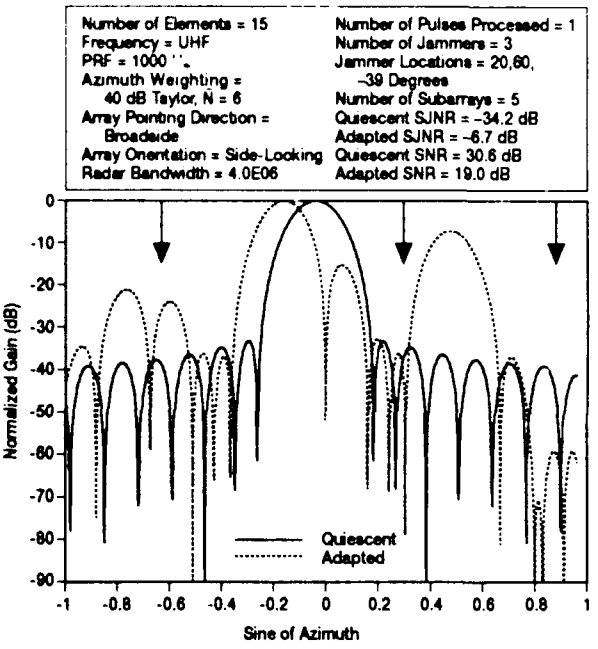

Figure 12. Effect of Grating Lobes on Adapted Gain Pattern and Performance

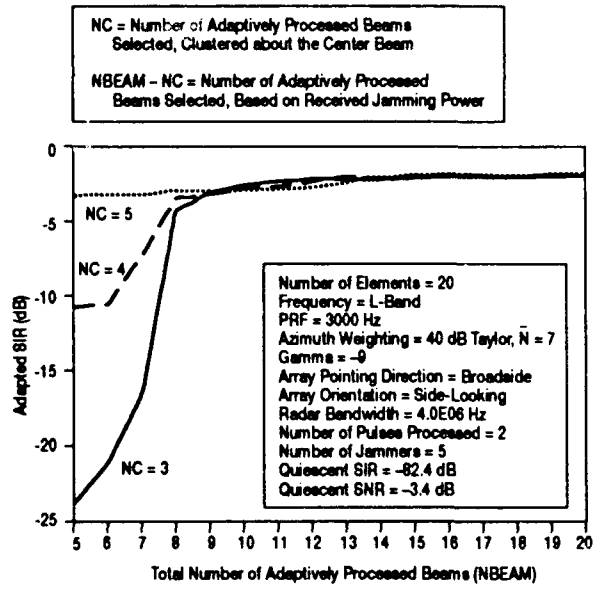

Figure 13. Effect of Beam Space Processing on Adapted Signal-to-Interference Ratio